Article

Current Biology

Bacterial hitchhikers derive benefits from fungal housing

Graphical abstract

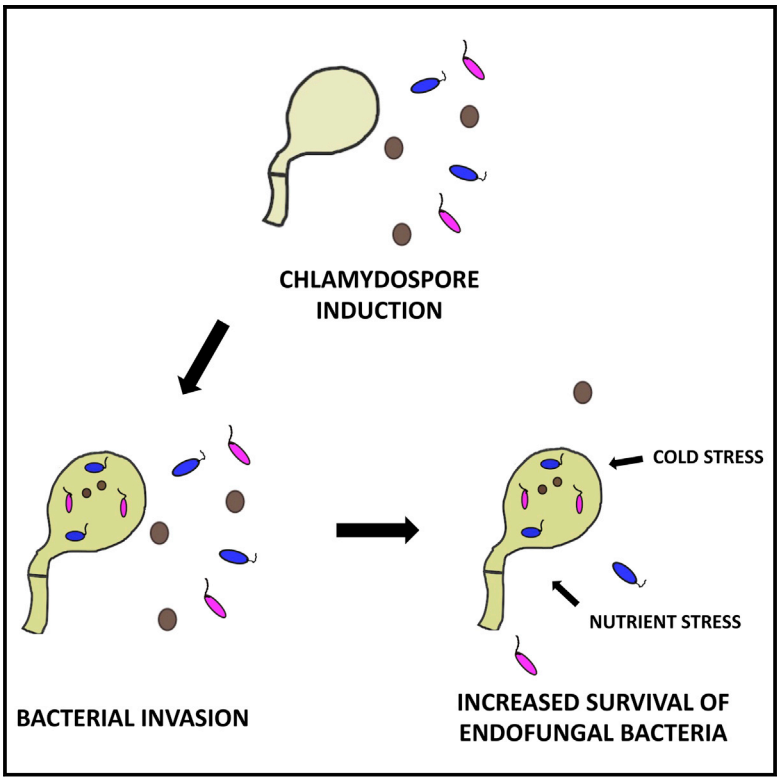

Highlights

- Bacteria produce lipopeptides that can induce formation of fungal chlamydospores
- Gram negative bacteria increase in population sizes in fungal chlamydospores
- Internalization increases bacterial fitness when challenged with abiotic stresses
- Chlamydospores can harbor more than one bacterial species

Authors

Nandhitha Venkatesh, Claudio Greco, Milton T. Drott, Max J. Koss, Isabelle Ludwikoski, Nina M. Keller, Nancy P. Keller

Correspondence

npkeller@wisc.edu

In brief

Venkatesh et al. show that phylogenetically and ecologically diverse free-living bacteria are able to colonize fungal chlamydospores induced by bacterial lipopeptides. Bacterial hitchhikers are able to ingress chlamydospores induced by other bacterial species, and colonization provides the bacteria with survival advantages under abiotic stress.

Venkatesh et al., 2022, Current Biology *32*, 1523–1533
April 11, 2022
https://doi.org/10.1016/j.cub.2022.02.017

CellPress

Current Biology

CellPress

Article

Bacterial hitchhikers derive benefits from fungal housing

Nandhitha Venkatesh,[1] Claudio Greco,[2,4] Milton T. Drott,[3] Max J. Koss,[2] Isabelle Ludwikoski,[2] Nina M. Keller,[2] and Nancy P. Keller[2,3,5,*]

[1]Department of Plant Pathology, University of Wisconsin–Madison, Linden Dr., Madison, WI 53706, USA
[2]Department of Medical Microbiology and Immunology, University of Wisconsin–Madison, Linden Dr., Madison, WI 53706, USA
[3]Department of Bacteriology, University of Wisconsin–Madison, Linden Dr., Madison, WI 53706, USA
[4]Present address: Department of Molecular Microbiology, John Innes Centre, Colney Ln., Norwich NR4 7UH, UK
[5]Lead contact
*Correspondence: npkeller@wisc.edu
https://doi.org/10.1016/j.cub.2022.02.017

SUMMARY

Fungi and bacteria are ubiquitous constituents of all microbiomes, yet mechanisms of microbial persistence in polymicrobial communities remain obscure. Here, we examined the hypothesis that specialized fungal survival structures, chlamydospores, induced by bacterial lipopeptides serve as bacterial reservoirs. We find that symbiotic and pathogenic gram-negative bacteria from non-endosymbiotic taxa enter and propagate in chlamydospores. Internalized bacteria have higher fitness than planktonic bacteria when challenged with abiotic stress. Further, tri-cultures of *Ralstonia solanacearum*, *Pseudomonas aeruginosa*, and *Aspergillus flavus* reveal the unprecedented finding that chlamydospores are colonized by endofungal bacterial communities. Our work identifies a previously unknown ecological role of chlamydospores, provides an expanded view of microbial niches, and presents significant implications for the persistence of pathogenic and beneficial bacteria.

INTRODUCTION

Bacterial fitness and persistence, although well studied in monoculture populations,[1,2] are relatively underexplored in polymicrobial environments. Endofungal bacteria are characterized by their ability to enter fungal cells, allowing them to engage in a specialized type of bacterial-fungal interaction (BFI) that has been described in numerous ecosystems. These bacteria, first described as bacteria-like organisms in spores of *Endogone* sp.,[3] are largely found in two taxa, Betaproteobacteria and Mollicutes, and primarily associate with the Mucoromycota, a clade of early-diverging fungi that includes mycorrhizal spp.[4–6] Historically, endofungal BFIs were thought to be specialized interactions that co-evolved between specific species and endofungal bacteria were identified upon visual observation of fungal isolates.[6–9] However, recent studies have identified non-obligate endofungal bacteria in Ascomycete and Basidiomycete fungi,[10–12] including cases where bacteria become intracellular fungal occupants when co-cultured *in vitro*,[12,13] colonize non-host fungi,[14] and include lineages not conventionally regarded as endosymbionts.[15] In a shift from classical interpretation, these studies support the idea that non-specific facultative associations may occur in nature.[16] However, direct evidence showing conventionally non-endosymbiotic bacteria adopting an endofungal lifestyle is exceedingly rare.

Here, we addressed the hypothesis that, in contrast to prevailing assumptions, bacterial ingress and survival in fungal tissue are common and mediated by lipopeptide signaling molecules. Building from our previous unexpected finding that the bacterial wilt-disease pathogen *Ralstonia solanacearum* adopts an endofungal lifestyle in fungal chlamydospores (multinucleate hyphal swellings with highly chitinous cell wall and lipid accumulation,[13,17] which function as survival structures[18,19]), we examined the outcomes of co-culturing diverse bacteria with the representative fungal partner *Aspergillus flavus*. We show that ralsolamycin (RM) and fengycin, lipopeptides produced by *R. solanacearum* (Rs)[13,17] and *Bacillus* spp.,[20–22] respectively, facilitate chlamydospore invasion by taxonomically diverse gram-negative, but not gram-positive, free-living bacteria. Furthermore, the internalized bacteria realize survival advantages in response to specific environmental stressors. We discover that chlamydospores can serve as a reservoir for bacterial communities as demonstrated by co-invasion of fungal structures by Rs and *Pseudomonas aeruginosa*. Arrival time influences chlamydospore colonization, with an advantage conferred to the founding bacterium. Our results identify a previously unrecognized BFI—one that we suggest represents an unrealized symbiotic archetype—that can facilitate bacterial fitness and persistence.

RESULTS

A model system to study facultative endofungal associations

Although we previously found that RM induces chlamydospore formation across all filamentous taxa examined to date (>30 species in Mucoromycota, Ascomycota, and Basidiomycota[13]), for consistency in all of the following experiments, *A. flavus* was

chosen as the fungal host, because it is a ubiquitous soil saprotroph, a plant pathogen of concern particularly for its ability to produce aflatoxin, and produces large, hyaline chlamydospores that are convenient for imaging endofungal bacteria. Two strains of Rs, the RM-producing wild-type (WT) and the RM-deletion mutant (Δ*rmyA*), were used to promote or not promote (respectively) chlamydospore formation in *A. flavus*.

Time-lapse imaging of *A. flavus* germlings exposed to WT Rs supernatant showed that chlamydospores differentiate from mature hyphal cells (Figure 1A; Video S1). Germlings of *A. flavus* treated with a concentration gradient of purified RM showed that chlamydospore formation was observed even at the lowest concentration tested (~15 nM) (Figure 1B). The number of chlamydospores produced by *A. flavus* was dependent on RM concentration (one-way ANOVA $p = 0.0058$; Figure 1B).

In order to observe gross-colony phenotypes of *A. flavus* in response to localized exposure of RM, the growing edge of the fungal thallus was exposed to varying RM concentrations. Hyphal extension was inhibited at RM concentrations higher than 1 μM (Figure 1C). Conidial production was stimulated at 1 and 0.1 nM (Figure 1C). Chlamydospores exposed to 16 μM (or 20 μg/mL) RM (the highest concentration detected in WT Rs supernatant) were viable, as indicated by a negative propidium iodide stain (Figure 1D) and successful germination.[13] These results show that RM mediates several developmental programs in the fungus but consistently induces viable chlamydospores at a wide range of concentrations, including those substantially lower than what the bacterium secreted in cultures (~16 μM).

A previous study from our group showed that WT Rs cells were found abundantly inside fungal chlamydospores, whereas Δ*rmyA* cells did not induce chlamydospores and were only rarely observed in the fungal hyphae.[13] In order to further verify that RM does indeed facilitate invasion of fungal structures, Rs was recovered from co-cultures by homogenization of fungal material after washing and agitation to remove external bacteria. Remaining bacteria were quantified by dilution plating on a bacterial-selective medium (Figure S1A). A significantly higher bacterial recovery ($p < 0.0001$) was obtained in WT co-cultures compared with Δ*rmyA* co-cultures (Figure 2D). WT and Δ*rmyA* Rs did not show significantly different growth dynamics (Figure S2A). For the rest of the text, the term "co-culture" is used for all two-way co-culture systems, i.e., a single bacterium interacting with a single fungal species.

Ralsolamycin enables colonization of chlamydospores by phylogenetically diverse bacteria

Adapting the above-described system for Rs colonization of *A. flavus* chlamydospores, we assessed if RM could enable the colonization of chlamydospores by phylogenetically diverse bacterial species, including primarily plant and human pathogens, as well as a nitrogen-fixing bacterium (see key resources table). We first confirmed that the supernatants did not affect bacterial viability with growth curves (Figure S2B), OD measurements (Figure S2C), and spot plating (data not shown) for each bacterial species cultured in WT or Δ*rmyA* supernatant. Bacteria were co-cultured with *A. flavus* and treated with supernatants of WT or Δ*rmyA* Rs or media control (Figure 2A). Chlamydospores were routinely observed in treatments with WT supernatant, whereas no chlamydospores were observed in treatments with Δ*rmyA* supernatant or media control (Figure S3B). In the co-cultures exposed to WT supernatant, chlamydospores were colonized by all gram-negative bacteria tested (Figures 2C and S3C), none of which have been previously reported to invade fungal cells. We also verified the ability of Δ*rmyA* Rs cells to invade chlamydospores induced by treatment with WT Rs supernatant (Figure S3D). In contrast to gram-negative bacteria, no gram-positive bacteria were found to enter chlamydospores. To further quantify the extent of invasion, we recovered *P. aeruginosa* from fungal mycelia after co-cultures were treated with WT or Δ*rmyA* supernatant (Figure 2B). A significantly higher recovery of *P. aeruginosa* cells was obtained from WT supernatant-treated co-cultures ($p = 0.0009$) (Figure 2E).

To confirm that bacterial invasion is the direct result of RM activity, *P. aeruginosa* was co-cultured with *A. flavus* with 0.125 μM purified RM (Figures S4A–S4C) or with methanol as the carrier control. Conversely, to identify whether a lack of invasion by gram-positive bacteria was due to confounding factors in the supernatant, we co-cultured *Listeria monocytogenes* and *C. michiganensis* in the presence of purified RM. Chlamydospore colonization with pure RM was consistent with results obtained with supernatant exposure (Figure S3A). Non-RM-producing bacteria that adopt endofungal lifestyles in the presence of RM are from here on termed "hitchhikers" and RM-producing Rs is termed "invader."

We could not find any literature reports of chlamydospore-invading gram-negative bacteria outside of the known endosymbiotic genus, a *Trinickia* sp.,[12] and our previous reports of Rs.[13,17] Although *Pseudomonas* spp. attach to *Fusarium* chlamydospores, inferences of invasion have so far been anecdotal.[23] A phylogenetic analysis based on 16S rRNA sequences (Figure S3E) showed that *Herbaspirillum* sp. B501 (and Rs) are closely related to known endofungal bacteria but that other hitchhikers, such as *P. aeruginosa* and *Escherichia coli*, as well as a few other endohyphal bacteria identified in other studies, do not segregate with the endofungal clade. Therefore, we conclude that RM can facilitate invasion of chlamydospores by bacteria that are phylogenetically distinct from known endofungal species. Overall, the results from our microscopic and physiological analyses demonstrate that RM enables chlamydospore colonization by ecologically and phylogenetically diverse, free-living gram-negative bacteria, including those with no known history of endofungal lifestyles.

Internalized invaders and hitchhikers realize fitness advantages under starvation

As chlamydospores are rich in glycogen[24] and lipid bodies,[13] we hypothesized that bacteria inside chlamydospores would have higher fitness (defined as an increase in population size of viable bacterial colony forming units [CFUs] post stress) than free living bacteria when starved for nutrients. Figure 3A depicts the setup for the bacterial fitness tests. We first asked if WT Rs would have higher fitness than the Δ*rmyA* mutant in *A. flavus* co-culture as only WT cells can colonize chlamydospores. Both WT and Δ*rmyA* Rs had reduced fitness in starved pure culture (Figure S5A). WT Rs in co-culture showed higher fitness than Δ*rmyA* cells in co-culture (two-way ANOVA, $p = 0.0015$; Figure 3B). Notably, starved chlamydospore co-cultures

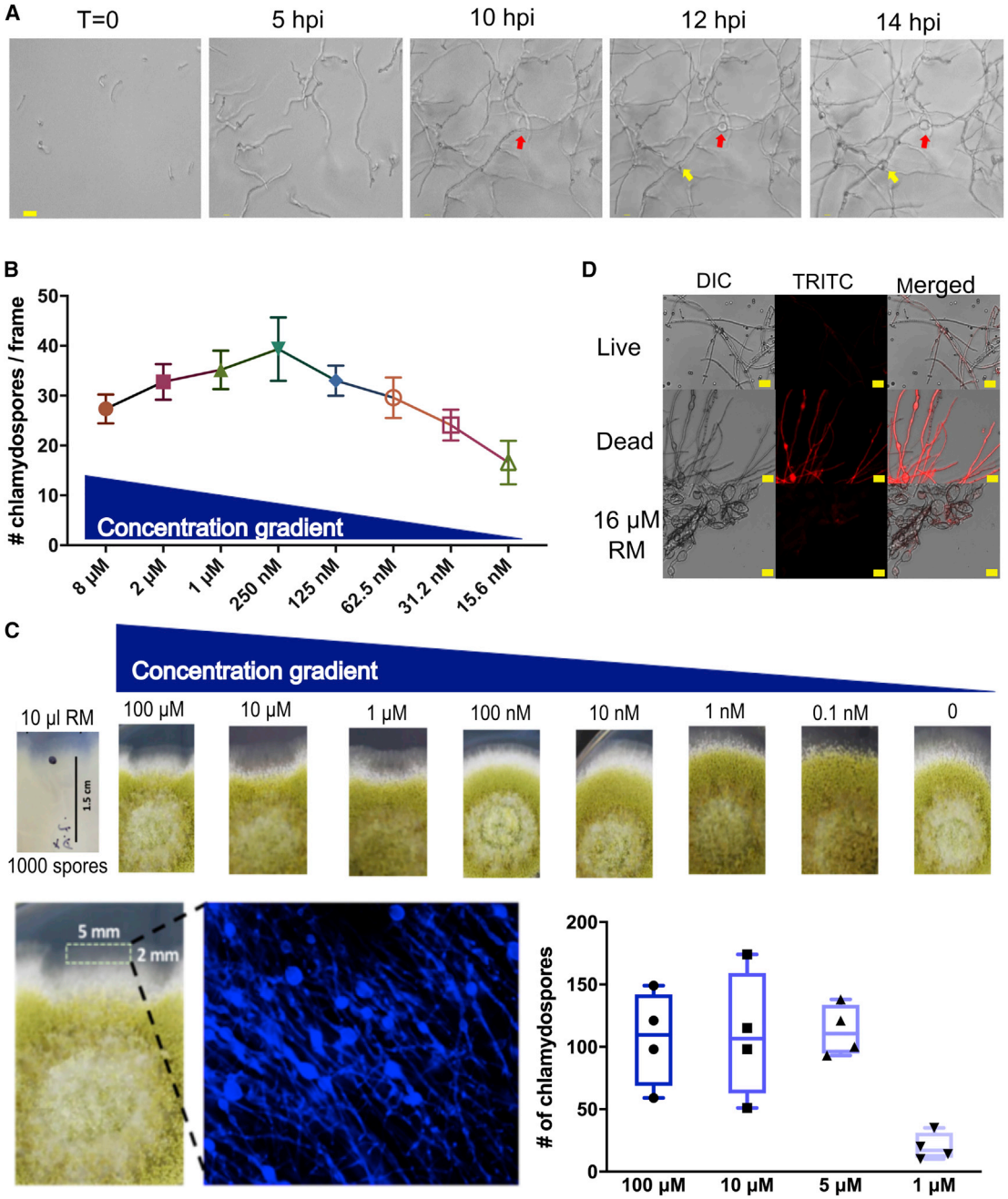

Figure 1. Ralsolamycin induces chlamydospore formation

(A) Time-lapse microscopy of *Aspergillus flavus* germlings treated with supernatants from *R. solanacearum* shows that mature hyphal cells are reprogrammed to form chlamydospores (each set of colored arrow follows formation of a given chlamydospore). Scale bar, 20 µm. See Video S1.

(B and C) *A. flavus* germlings (B) or mycelia (C) were exposed to different concentrations of purified ralsolamycin for 2 and 4 days, respectively, at 30°C. Methanol was used as the carrier control. Interaction zones identified in (C-bottom) with the white box (5 × 2 mm) were excised and stained with 1 mg/mL calcofluor white. Fluorescent imaging was performed to see defined and distinctive chlamydospores. The number of chlamydospores were then manually counted with the "cell counter" option on Fiji. For (B), 12 frames per concentration were counted; one-way ANOVA was performed with Bonferroni correction, $p = 0.0058$. For (C), $n = 4$ replicates × 6 frames per replicate; Kruskal-Wallis test was performed with Dunn's correction, $p = 0.0193$.

(D) *A. flavus* germlings were exposed to 16 µM ralsolamycin with methanol as the control (live) and incubated for 3 days at 30°C. RM-treated hyphae exposed to 15% H_2O_2 served as the dead control. All samples were stained with propidium iodide (25 µg/mL) for 10 min and imaged under the TRITC channel. Scale bar, 20 µm.

Also see Figure S4 for details and properties of purified RM.

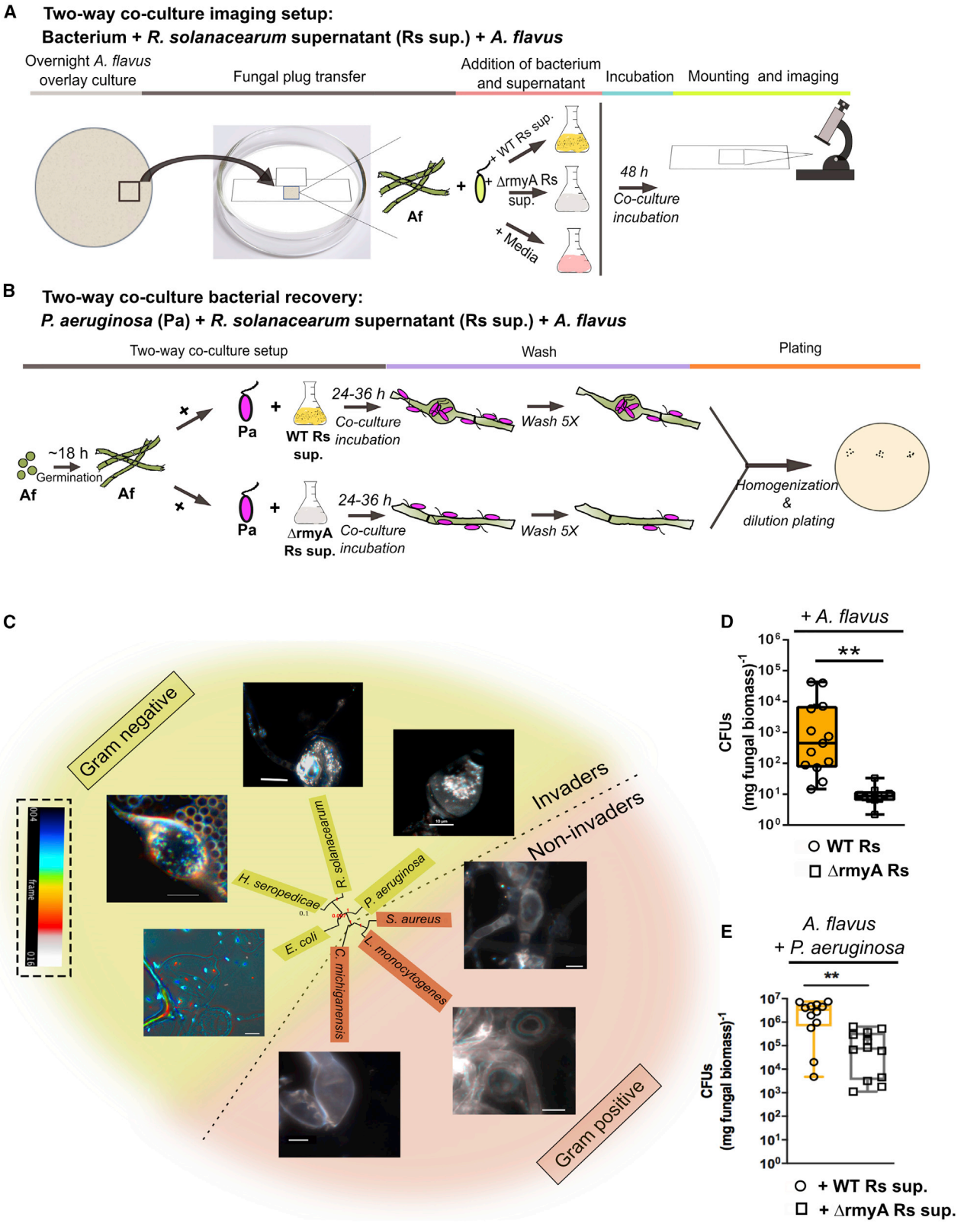

Figure 2. Bacteria with previously unreported endofungal lifestyles invade chlamydospores in the presence of RM

(A) This panel shows the schematic for all co-culture imaging analyses. All bacteria were fluorescently tagged.

(B) This panel depicts experimental design for recovery of *Pseudomonas aeruginosa* from co-cultures.

(legend continued on next page)

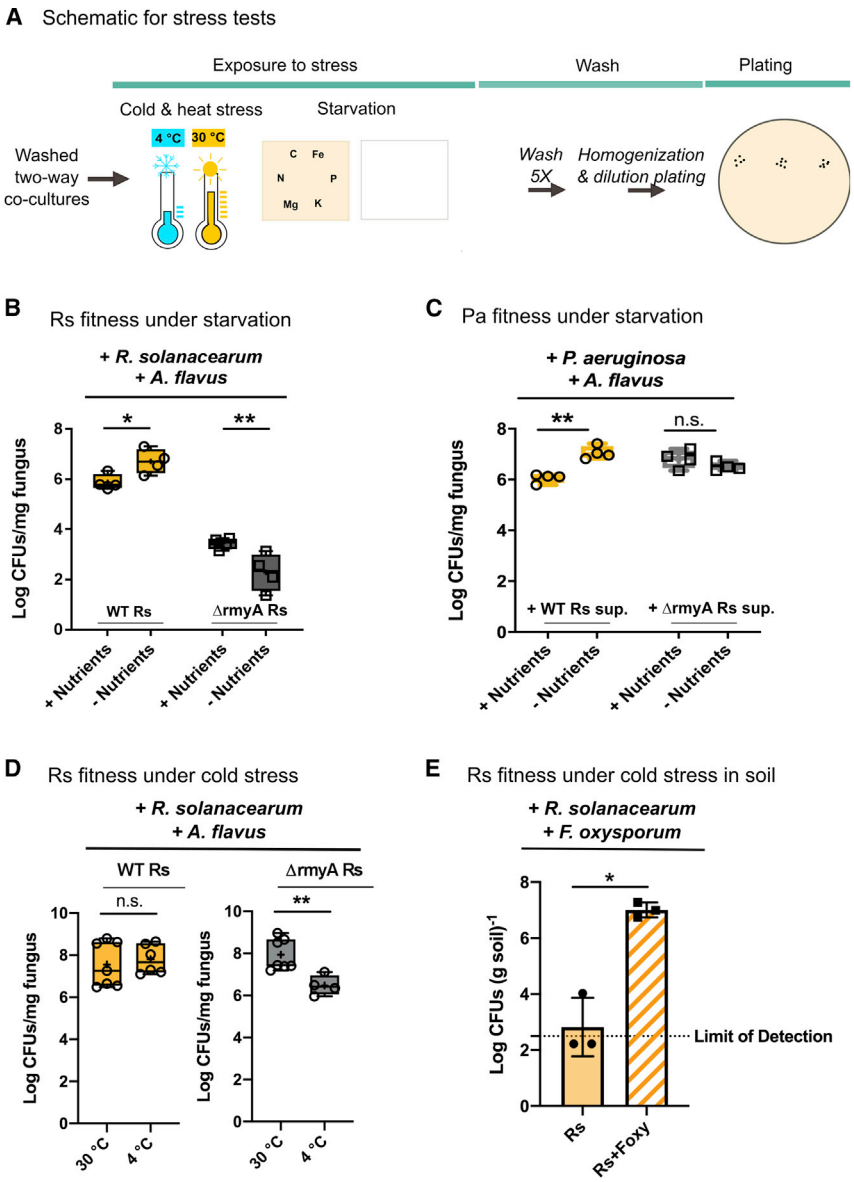

Figure 3. Bacteria derive advantages from endofungal lifestyle

(A) Schematic showing methods for stress tests. Control treatments are shown in Figures S5–S7. All graphs show bacterial colony forming units (CFUs) per mg fungal biomass from co-cultures with *A. flavus* (+ *A. flavus*). For all graphs, n = 4–8 replicates × 3 co-culture setups pooled per replicate. CFUs of WT or Δ*rmyA R. solanacearum* from co-cultures were individually compared between treatments with and without stress.

(B) Population size of *R. solanacearum* in co-cultures with *A. flavus* under conditions of starvation. Two-way ANOVA p = 0.0015; Holm Sidak's post hoc p = 0.0326 (+WT Rs sup) and p = 0.0113 (-+ΔrmyA Rs sup).

(C) Shows the population size of *P. aeruginosa* cells in co-culture *with A. flavus* when treated with Rs supernatant. Two-way ANOVA interaction p = 0.0002; Holm Sidak's post hoc p = 0.0001 (+WT Rs sup) and p = 0.1115 (+ΔrmyA Rs sup).

(D) Shows population size of *R. solanacearum* post cold stress in chlamydospore co-cultures (yellow) and the control (gray). VBNC *R. solanacearum* cells are resuscitated with catalase treatment. The data did not satisfy fit two-way ANOVA assumptions model. Mann-Whitney test was performed for pairwise comparisons. WT Rs: p = 0.7308 and ΔrmyA Rs p = 0.0061.

(E) Shows *R. solanacearum* population size in co-cultures with *F. oxysporum* in soil microcosms exposed to prolonged cold. n = 3; unpaired t test with Welch's correction was performed with p = 0.0156. Error bars show standard deviation.

See Figure S1B for schematic.

resulted in higher recovery of CFUs of WT bacterium than from nutrient-sufficient conditions (p = 0.0326; Figure 3B [yellow boxes]). This demonstrates that the endofungal lifestyle in chlamydospores offers fitness advantages to the bacterium under starvation. We also observed that starved WT Rs cells are able induce chlamydospores (although in lower numbers than unstarved cells) (Figure S6A). The proportion of chlamydospores colonized by starved Rs cells was not significantly different from that of unstarved cells (Figure S6B) in the presence of exogenous RM.

To examine if such nutritional advantages are realized by hitchhikers in fungal chlamydospores, we co-cultured *P. aeruginosa* with *A. flavus* in WT or Δ*rmyA* Rs supernatant under starvation. In chlamydospore co-cultures (Figure 3C [yellow box]), *P. aeruginosa* realized higher fitness/survival under starvation compared with chlamydospore-absent co-cultures (two-way ANOVA p = 0.0002; Figures 3C [gray box] and S7A). The fitness advantage was not observed in pure cultures of *P. aeruginosa* (Figure S5B).

To understand if the fitness advantage is conferred only to internalized bacteria, or if other aspects of fungal growth and response to the lipopeptides contributed to bacterial

(C) Fluorescent imaging with z-stacks (8–12 slices) showed bacteria in multiple slices. Fiji depth coloring feature was used to color each slice and the colored slices were re-assembled to form the images shown. The inset on the left shows the depth color scale—blue-colored bacteria are present in deeper layers than white-colored bacteria. Scale bar, 10 μm. Chlamydospore invaders and hitchhikers (indicated as "invaders") are highlighted with a yellow background, whereas non-invaders are highlighted pink. See Figures S2 and S3 for controls.

(D) CFUs of *R. solanacearum* isolated from co-cultures with *A. flavus*; n = 16 (WT) or 12 (Δ*rmyA*). The distribution was non-normal based on Shapiro-Wilk test, non-parametric Mann-Whitney U test was performed with p < 0.0001. See Figures S1A and S1C for schematic.

(E) CFUs of *P. aeruginosa* isolated from co-cultures with *A. flavus* treated with WT or Δ*rmyA* Rs supernatant. n = 12; the distribution was not normal based on Shapiro-Wilk test, non-parametric Mann-Whitney U test was performed (p = 0.0009).

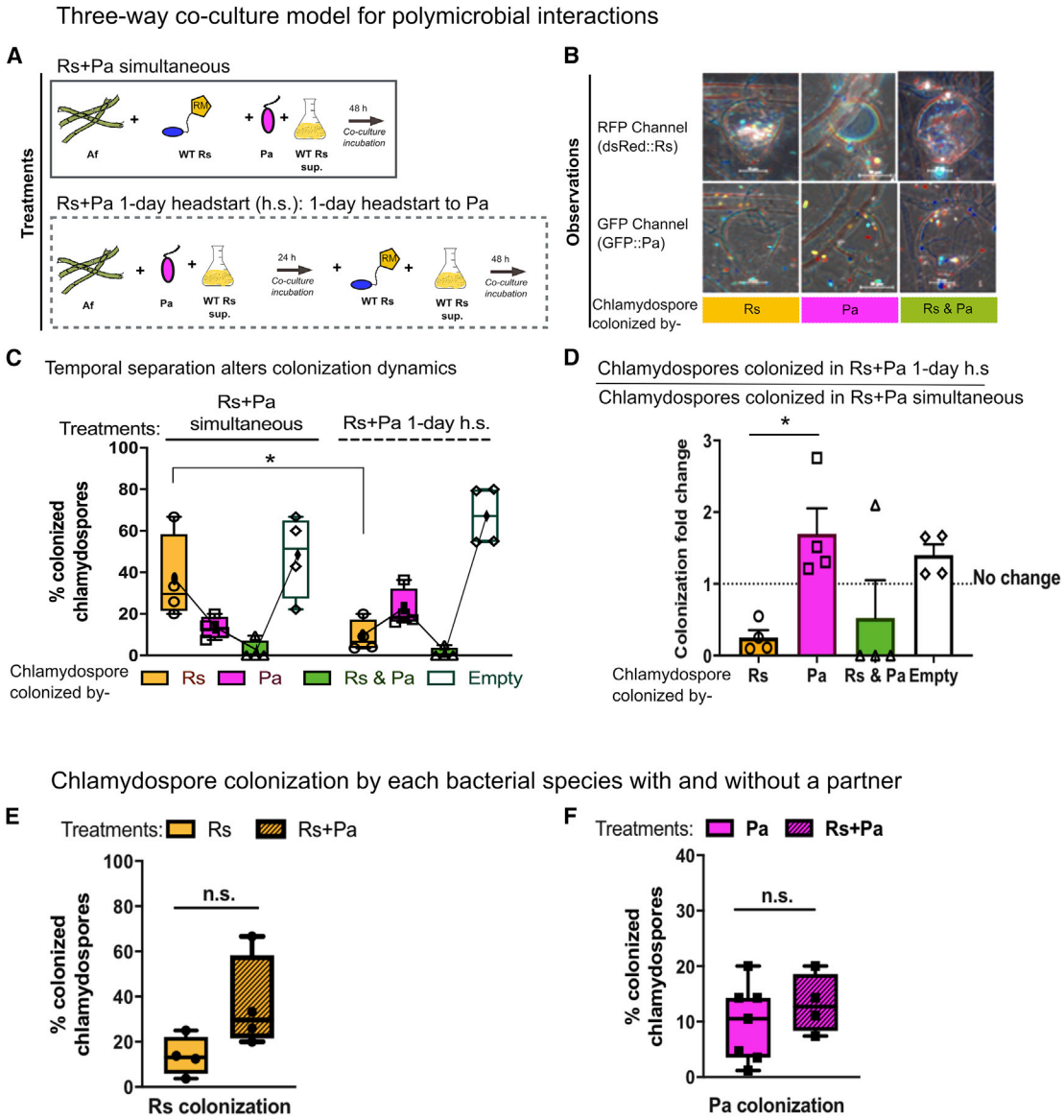

Figure 4. Chlamydospores support an endofungal microbiome and temporal changes alter colonization dynamics in polymicrobial environments

The polymicrobial setup here includes *R. solanacearum* (Rs - only seen in RFP channel) and *P. aeruginosa* (Pa - only seen in GFP channel) interacting with *A. flavus*.

(A) This panel explains the design for a three-way co-culture system with two bacteria and *A. flavus*. The two bacteria were simultaneously co-inoculated with the fungus (solid outline box) or *P. aeruginosa* given a 1-day head start (dotted outline box).

(B) This panel shows the different chlamydospore-colonization patterns observed in the three-way co-culture system. Chlamydospores where only Rs was present (yellow), where only Pa was present (pink) and where both (green) were present were observed. The relative proportion of chlamydospores showing each of the colonization types were quantified in (C).

(C) Chlamydospores of each colonization type were compared between simultaneous introduction of bacteria and a 1-day head start (h.s.) to *P. aeruginosa* (C) (two-way ANOVA p = 0.0067 with Holm-Sidak's post hoc p = 0.0192).

(D) Relative colonization of bacteria with and without head start suggest that *P. aeruginosa* cells gain and *R. solanacearum* cells lose colonization advantages when Pa is given a 1-day head start (one-way ANOVA p = 0.0270 and Tukey's post hoc, *p = 0.0403).

(E and F) These panels compare the colonization abilities of each bacterial spp. between two-way and three-way interactions for *R. solanacearum* and *P. aeruginosa*, respectively. n = 4. t test with Welch's correction was performed that showed no significant differences in colonization behavior: (E) Rs: p = 0.1143 and (F) Pa: p = 0.3855.

fitness, we exposed co-cultures of a non-invader bacterium, *L. monocytogenes*, to WT or Δ*rmyA* Rs supernatant under starvation. This non-invading bacterium did not realize fitness advantages associated with chlamydospore formation (two-way ANOVA p = 0.8851; Figure S7B). Overall, the data show that endofungal invaders and hitchhikers in chlamydospores

Table 1. Lipopeptides that induce chlamydospores or chlamydospore-like structures in fungi

Lipopeptide	Natural/synthetic chemical	Chlamydospores or chlamydospore-like hyphal swellings reported in-	Properties
Fengycin A	natural (produced by *Bacillus* spp.)[30]	*Magnaporthe oryzae*,[21] *Fusarium solani*[31]	antifungal, antibacterial, and biosurfactant[32]
Simplicilliumtide J[33]	natural (from the deep-sea-fungus *Simplicillium obclavatum*)	*Aspergillus versicolor and Curvilaria australiensis*	antifungal
Verlamelin A[33]	natural (from the deep-sea-fungus *Simplicillium obclavatum*)	*Aspergillus versicolor and Curvilaria australiensis*	antifungal
Viscosinamide[34]	natural (from *Pseudomonas fluorescens*)	*Rhizoctonia solani*	antifungal and surfactant
Tensin[35]	natural (from *Pseudomonas fluorescens*)	*Rhizoctonia solani*	antifungal and surfactant
Anidulafungin	semi-synthetic (precursor from *A. nidulans*[36])	*Candida* sp.[37]	antifungal[36]
Micafungin	semi-synthetic (precursor from *Coleophoma empetri*[38])	*Candida albicans*; in infected lung tissue from neutropenic rabbits[39]	antifungal[36]

realize fitness advantages under starvation conditions that are not accessible to non-invading bacteria.

Internalization enhances *Ralstonia solanacearum* survival in cold temperatures

Chlamydospores contribute to survival of fungi in soil due to the ability of these structures to withstand extreme temperatures.[18,19] Although plant tissues are thought to be the main reservoir of overwintering Rs, persistence of this bacterium in agricultural soils even after herbicide treatment has raised questions about other mechanisms of overwintering.[25] Therefore, we tested if Rs survival in soil could be partially explained by the ability of this bacterium to invade chlamydospores. To emulate cold stress, co-cultures of WT or *ΔrmyA* Rs were grown in minimal media and incubated for 30 days at 4°C (cold stress) or 30°C (control) (Figure 3A). Under cold stress, Rs cells have been shown to go into a viable but non culturable (VBNC) state,[26] which can be resuscitated by treatment with catalase.[27] We found that bacteria did enter the VBNC state in both pure cultures and co-cultures at 4°C, as no colonies were recovered unless treated with catalase. Upon resuscitation, WT Rs co-cultures showed significantly higher survival under cold stress than Δ*rmyA* co-cultures at 4°C (WT Rs p = 0.7308; Δ*rmyA* Rs p = 0.0061; Figure 3D [compare yellow versus gray boxes]). Notably, there is a significant reduction in bacterial fitness in co-cultures when chlamydospores are absent (p = 0.0061) (Figure 3D [gray boxes]). The survival advantage was not observed in pure cultures of Rs (Figure S5C).

The enhanced survival of WT Rs co-culture presented a groundbreaking view of how this phytopathogen may survive cold temperatures in the soil microbiome. To emphasize that the patterns we observed in our model BFI system occur between plant pathogens relevant to economically important disease systems, we tested the overwintering ability of Rs in soil microcosms maintained at 4°C for 3 weeks with *Fusarium oxysporum*, a soilborne fungal phytopathogen that also causes wilt disease (Figure S1B). This fungal partner was chosen because Rs and *F. oxysporum* infect similar hosts, colonize the plant xylem, and Rs invades chlamydospores of *Fusarium fujikuroi*.[17] Our results show that a significantly higher number of bacterial colonies were recovered from co-cultures compared with bacterial monocultures in the soil microcosm (p=0.0156; Figure 3E). Taken together, we speculate that Rs may overwinter in fungal survival structures present in agricultural soil, which warrants future experimentation in natural settings. These findings also emphasize the need for a prudent re-examination of current management strategies designed to manage bacterial wilt disease.

Bacterial co-habitation of chlamydospores

We next considered the possibility that chlamydospores could harbor more than one bacterial species. A three-way co-culture system was developed with *A. flavus*, *R. solanacearum*::dsRed (observed only in the red fluorescent protein channel), and *P. aeruginosa*::GFP (observed only in the green fluorescent protein channel) with Rs supernatants (Figure 4A [solid outline box, Rs+Pa simultaneous]). Imaging analyses after 48 h post incubation revealed that ~36% of chlamydospores were colonized by only Rs, ~13% by only *P. aeruginosa*, and 2.4% by both bacteria (Video S2), whereas ~50% remained empty (Figures 4B and 4C [left panel]). Whereas there is a smaller percentage of colonization by both bacteria, suggesting a somewhat rare event, this percentage is still large if actualized in natural environments. Together, these results demonstrate that different bacterial species can colonize a given chlamydospore.

Microbial community dynamics often shift based on the order of appearance, with early-arriving organisms influencing community assembly.[28] Thus, we considered that the arrival time of bacteria could influence their ability to invade and colonize chlamydospores. To address this, *P. aeruginosa* was given a head start of 24 h before addition of Rs cells (Figure 4A [dotted outline box]). The dynamics of colonization shifted in response to the head start provided to *P. aeruginosa*, with *P. aeruginosa* colonizing more chlamydospores (~22%) than Rs (9%) (Figure 4C [right panel]). Comparison of colonization rates show that Rs colonization is significantly reduced when it is introduced after *P. aeruginosa* (two-way ANOVA p = 0.0067 with Holm-Sidak's post hoc p = 0.0192; Figure 4C) (one-way ANOVA p = 0.0270 and Tukey's post hoc, p = 0.0403; Figure 4D), indicating that colonization of chlamydospores is influenced by the arrival time of microbes. Colonization of a single chlamydospore by both microbes remained unchanged.

We next asked whether a given bacterial species is more or less likely to enter a chlamydospore in the presence of

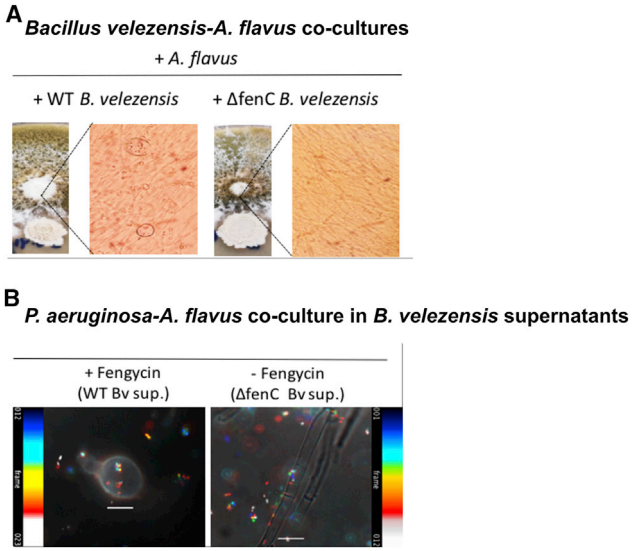

Figure 5. Fengycin, a bacterial lipopeptide, induces chlamydospores and facilitates bacterial invasion

(A) *A. flavus* and WT or Δ*fenC B. velezensis* were co-cultured with *A. flavus* on LB for 1 week. Interaction zones were imaged to identify chlamydospores only present in WT co-culture.

(B) Co-cultures of *P. aeruginosa* with *A. flavus* in WT Bv supernatant shows bacteria inside chlamydospores, whereas no bacterial invasion is observed in treatment with Δ*fenC* Bv supernatant. Scale bar, 10 μm.

Related to Figure S2D.

another bacterium. We, therefore, compared the percentage of chlamydospores colonized by each bacterium in the two-way versus the three-way co-culture. Colonization of chlamydospores by either bacterium was not significantly different in the presence of a bacterial partner (Figures 4E [Unpaired t test p = 0.3868] and 4F [Unpaired t test p = 0.1143]).

Collectively, our results provide insights into the possible dynamics of BFIs in polymicrobial settings. In the presence of RM, *A. flavus* chlamydospores can host a bacterial community whose assembly is likely influenced by the arrival time of the bacteria.

Conservation of lipopeptide-mediated bacterial ingress of chlamydospores

Numerous bacteria and fungi produce lipopeptides,[29] and some of these lipopeptides have been reported to induce chlamydospore formation but have not been examined for bacterial ingress (Table 1). Similar to RM, these lipopeptides show concentration-dependent antifungal and/or biosurfactant activity, as verified with an oil-spreading assay (Figures 1C and S4D). Predicting that lipopeptide-facilitated fungal invasion could be common in nature, we asked if fengycin, a lipopeptide produced by the gram-positive *Bacillus velezensis*[20] (Table 1), could induce chlamydospores and subsequent invasion by gram-negative bacteria. Co-cultures of *A. flavus* with WT B. *velezensis* showed chlamydospore formation, whereas no chlamydospores were observed in co-cultures with Δ*fenC* B. *velezensis* (a mutant unable to produce fengycin[20]) (Figure 5A). To test the hypothesis that fengycin, similar to RM, promotes bacterial invasion of fungal tissue, a two-way co-culture system was developed with *P. aeruginosa* and *A. flavus* treated with B. *velezensis* WT or Δ*fenC* supernatants (Figure S2D). Imaging analyses showed that chlamydospores were colonized by *P. aeruginosa* in WT supernatant treatment, whereas no chlamydospores or invasion was observed in co-cultures with Δ*fenC* treatments (Figure 5B). Our results show that fengycin, similar to RM, facilitates bacterial invasion into fungal chlamydospores.

DISCUSSION

Here, for the first time, we provide evidence that phylogenetically and ecologically diverse free-living bacteria, unrecognized for endofungal lifestyles, are able to colonize fungal chlamydospores induced by bacterial lipopeptides under *in vitro* conditions. This phenomenon is reminiscent of "cheating" for "public goods" described for bacterial populations.[40] For example, non-siderophore-producing pseudomonads realize fitness advantages of siderophores by co-occurring with siderophore-secreting genotypes[41] under carbon limitation.[42] Along similar lines, we find bacteria with vastly different lifestyles—the entero-invasive *E. coli*, the lung colonizing *P. aeruginosa*, and the free-living nitrogen-fixer *Herbaspirillum seropedicae*—become hitchhikers in the presence of bacterial lipopeptides and realize survival advantages associated with this ingress.

We propose that chlamydospore formation and bacterial invasion may occur across a wide variety of bacterial-fungal partners in diverse environments (Figure 6), which remains to be experimentally assessed. Lipopeptides have been identified from bacteria and fungi from various niches,[29,43–47] and genome analyses reveal extensive genetic potential for production of these molecules.[48–52] Several lipopeptides induce chlamydospores (Table 1) in diverse fungi.[13] Further, our data suggest that bacteria may derive significant survival advantages by utilizing lipopeptides to establish an endofungal lifestyle. Together, we speculate that these lipopeptide-mediated facultative endofungal interactions may occur in nature. Chlamydospores have been observed *in planta*,[19] *in vivo* in mice infected with *Candida*,[53] *Aspergillus*,[39] and *Fusarium* spp.[54] and reported in an AIDS patient,[55] in sputum[56] and from lung autopsies.[57] Our findings promote the possibility of endofungal-bacteria-enriched microbiomes, which not only requires consideration of combinatorial therapeutic and biocontrol strategies but also opens the door toward leveraging endofungal interactions for engineering efficient nitrogen fixation, bioremediation, and preservation of food products.

Although we examined several taxonomically and ecologically diverse bacteria, it is notable that all gram-negative, but no gram-positive bacteria, were able to colonize chlamydospores, suggesting a mechanism that may favor gram-negative bacteria under certain environmental conditions. We propose that survival advantages realized by endofungal invaders and hitchhikers relative to non-invading bacteria could alter the composition of microbial communities over time. Several studies have documented the selective effect of the mycosphere on soil bacteria (as reviewed in[58]). We speculate that this may be in part be due to selection for or against endofungal invaders and hitchhikers in the community.

Our findings that chlamydospores can host more than one bacterial species calls attention toward treating fungi acting

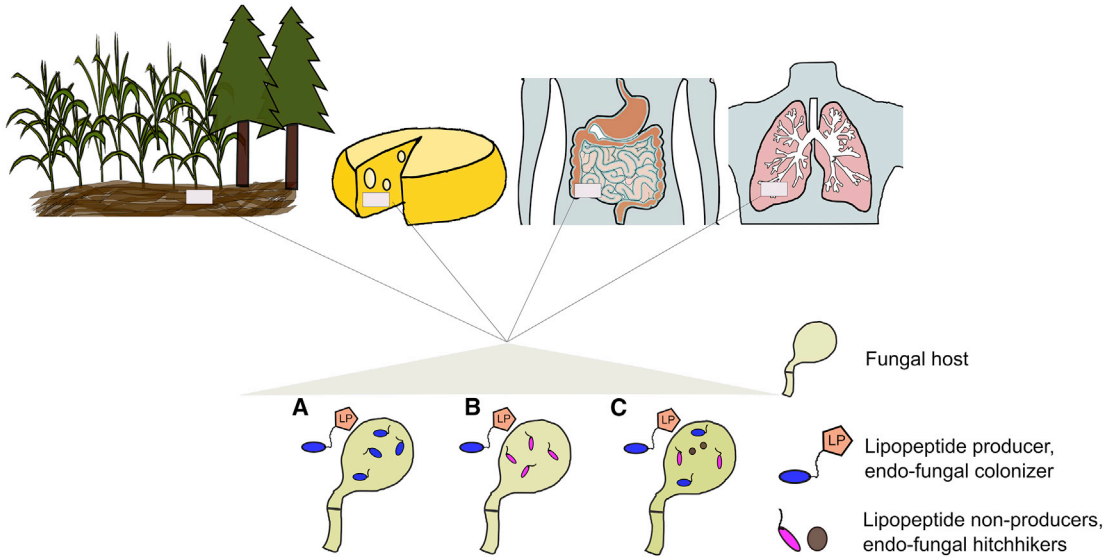

Figure 6. Proposed endofungal behavior in polymicrobial environments

(A and B) In varied microenvironments, such as the rhizosphere, cheese, human gut, and human lungs (left to right, top row), microbes perceive and interpret inter-kingdom signals. Lipopeptides (LP) secreted by bacteria and fungi result in bacterial invasion of fungal chlamydospores (green) by lipopeptide-producing bacteria (in blue, A) and hitchhikers (purple, B).

(C) Co-occurrence of multiple hitchhikers (purple and brown) and invaders results in the assembly of an endofungal-bacterial community.

as "meta-organisms"[4] supported by an earlier study that reported two different endobacteria in the spore of an arbuscular mycorrhizal fungus[59] (Figure 6). We speculate that endofungal microbiomes allow for intimate interactions among resident bacteria, as well as with the fungal host, which could promote not only the sharing of nutrients but also the exchange of genetic material (e.g., horizontal gene transfer, phage transfer, etc.). This work identifies chlamydospores as providing a protective habitat for multiple endofungal bacterial partners.

Endofungal invasion can offer advantages to the bacterial invaders and hitchhikers in environmental extremes. Although bacterial overwintering and survival in harsh environmental conditions have only been attributed to plants and plant material, for the first time, we show that endofungal invasion offers increased fitness to the invading bacterium under nutrient starvation and cold stress. Questions remain about the interdependencies in this interaction (i.e., how the microbes perceive and recognize the stress, mechanisms that bacteria employ to derive nutrition and protection inside chlamydospores, and how the fungus extends, limits, or shares nutrients to/with the bacteria), the fate of internalized bacteria upon chlamydospore germination, and the consequences on the fungal partner. In summary, results from this work present a shift in how we think of bacterial persistence and proposes a heretofore unknown ecological role for fungal chlamydospores in nature.

STAR★METHODS

Detailed methods are provided in the online version of this paper and include the following:

SUPPLEMENTAL INFORMATION

Supplemental information can be found online at https://doi.org/10.1016/j.cub.2022.02.017.

ACKNOWLEDGMENTS

This work was supported in part by the National Institute of Food and Agriculture, United States Department of Agriculture, Hatch project 1012878 to N.P.K; the National Institutes of Health under grant 5R01GM112739-06 and 5R01AI150669-02 to N.P.K.; and the UW-Madison Food Research Institute's E. Michael and Winona Foster Wisconsin Distinguished Fellowship Award to N.V. We thank Dr. Dirk Hoffmeister and Dr. Florian Baldeweg for providing the purified compound ralsolamycin. We thank the following people for their

generous sharing of microbial strains used in this study—Dr. Caitilyn Allen, Dr. Jean-Michel Ané, Dr. John-Demian Sauer, Dr. Rodney Welch, Dr. Christine Smart, Dr. Suzanne Fleiszig, Dr. Antonio Di Pietro, and Dr. John Helmann. Special thanks to Dr. Breanne Steffan for the review of this manuscript.

AUTHOR CONTRIBUTIONS

N.V., C.G., M.T.D., and N.P.K. developed and designed the experiments for the study. N.V., M.J.K., N.M.K., and I.L. performed the experiments. N.V., C.G., and N.P.K. analyzed and interpreted the data. N.V., I.L., and N.P.K. wrote the paper. All authors reviewed the paper.

DECLARATION OF INTERESTS

The authors declare no competing interests.

Received: May 12, 2021
Revised: October 14, 2021
Accepted: February 3, 2022
Published: March 1, 2022

REFERENCES

1. Gardner, A., West, S.A., and Griffin, A.S. (2007). Is bacterial persistence a social trait? PLoS One *2*, e752.
2. Kussell, E., Kishony, R., Balaban, N.Q., and Leibler, S. (2005). Bacterial persistence: a model of survival in changing environments. Genetics *169*, 1807–1814.
3. Mosse, B. (1970). Honey-coloured, sessile Endogone spores: II. Changes in fine structure during spore development. Archiv. Mikrobiol. *74*, 129–145.
4. Deveau, A., Bonito, G., Uehling, J., Paoletti, M., Becker, M., Bindschedler, S., Hacquard, S., Hervé, V., Labbé, J., Lastovetsky, O.A., et al. (2018). Bacterial-fungal interactions: ecology, mechanisms and challenges. FEMS Microbiol. Rev. *42*, 335–352.
5. Frey-Klett, P., Burlinson, P., Deveau, A., Barret, M., Tarkka, M., and Sarniguet, A. (2011). Bacterial-fungal interactions: hyphens between agricultural, clinical, environmental, and food microbiologists. Microbiol. Mol. Biol. Rev. *75*, 583–609.
6. Pawlowska, T.E., Gaspar, M.L., Lastovetsky, O.A., Mondo, S.J., Real-Ramirez, I., Shakya, E., and Bonfante, P. (2018). Biology of fungi and their bacterial endosymbionts. Annu. Rev. Phytopathol. *56*, 289–309.
7. Bianciotto, V., Bandi, C., Minerdi, D., Sironi, M., Tichy, H.V., and Bonfante, P. (1996). An obligately endosymbiotic mycorrhizal fungus itself harbors obligately intracellular bacteria. Appl. Environ. Microbiol. *62*, 3005–3010.
8. Ghignone, S., Salvioli, A., Anca, I., Lumini, E., Ortu, G., Petiti, L., Cruveiller, S., Bianciotto, V., Piffanelli, P., Lanfranco, L., and Bonfante, P. (2012). The genome of the obligate endobacterium of an AM fungus reveals an interphylum network of nutritional interactions. ISME J *6*, 136–145.
9. Lackner, G., Moebius, N., Partida-Martinez, L.P., Boland, S., and Hertweck, C. (2011). Evolution of an endofungal lifestyle: deductions from the *Burkholderia rhizoxinica* genome. BMC Genomics *12*, 210.
10. Shaffer, J.P., U'Ren, J.M., Gallery, R.E., Baltrus, D.A., and Arnold, A.E. (2017). An endohyphal bacterium (*Chitinophaga*, Bacteroidetes) alters carbon source use by *Fusarium keratoplasticum* (*F. solani* species complex, *Nectriaceae*). Front. Microbiol. *8*, 350.
11. Li, X.S., Sato, T., Ooiwa, Y., Kusumi, A., Gu, J.-D., and Katayama, Y. (2010). Oxidation of elemental sulfur by *Fusarium solani* strain THIF01 harboring endobacterium *Bradyrhizobium* sp. Microb. Ecol. *60*, 96–104.
12. del Barrio-Duque, A., Samad, A., Nybroe, O., Antonielli, L., Sessitsch, A., and Compant, S. (2020). Interaction between endophytic Proteobacteria strains and *Serendipita indica* enhances biocontrol activity against fungal pathogens. Plant Soil *451*, 277–305.
13. Spraker, J.E., Sanchez, L.M., Lowe, T.M., Dorrestein, P.C., and Keller, N.P. (2016). *Ralstonia solanacearum* lipopeptide induces chlamydospore development in fungi and facilitates bacterial entry into fungal tissues. ISME J *10*, 2317–2330.
14. Arendt, K.R., Hockett, K.L., Araldi-Brondolo, S.J., Baltrus, D.A., and Arnold, A.E. (2016). Isolation of endohyphal bacteria from foliar Ascomycota and *in vitro* establishment of their symbiotic associations. Appl. Environ. Microbiol. *82*, 2943–2949.
15. Hoffman, M.T., and Arnold, A.E. (2010). Diverse bacteria inhabit living hyphae of phylogenetically diverse fungal endophytes. Appl. Environ. Microbiol. *76*, 4063–4075.
16. Bonfante, P., Venice, F., and Lanfranco, L. (2019). The mycobiota: fungi take their place between plants and bacteria. Curr. Opin. Microbiol. *49*, 18–25.
17. Spraker, J.E., Wiemann, P., Baccile, J.A., Venkatesh, N., Schumacher, J., Schroeder, F.C., Sanchez, L.M., and Keller, N.P. (2018). Conserved responses in a war of small molecules between a plant-pathogenic bacterium and fungi. mBio *9*, e00820-18.
18. Son, H., Lee, J., and Lee, Y.-W. (2012). Mannitol induces the conversion of conidia to chlamydospore-like structures that confer enhanced tolerance to heat, drought, and UV in *Gibberella zeae*. Microbiol. Res. *167*, 608–615.
19. Francisco, C.S., Ma, X., Zwyssig, M.M., McDonald, B.A., and Palma-Guerrero, J. (2019). Morphological changes in response to environmental stresses in the fungal plant pathogen *Zymoseptoria tritici*. Sci. Rep. *9*, 9642.
20. Cao, Y., Pi, H., Chandrangsu, P., Li, Y., Wang, Y., Zhou, H., Xiong, H., Helmann, J.D., and Cai, Y. (2018). Antagonism of two plant-growth promoting *Bacillus velezensis* isolates against *Ralstonia solanacearum* and *Fusarium oxysporum*. Sci. Rep. *8*, 4360.
21. Zhang, L., and Sun, C. (2018). Fengycins, cyclic lipopeptides from marine *Bacillus subtilis* strains, kill the plant-pathogenic fungus *Magnaporthe grisea* by inducing reactive oxygen species production and chromatin condensation. Appl. Environ. Microbiol. *84*, e00445.
22. Steller, S., Vollenbroich, D., Leenders, F., Stein, T., Conrad, B., Hofemeister, J., Jacques, P., Thonart, P., and Vater, J. (1999). Structural and functional organization of the fengycin synthetase multienzyme system from *Bacillus subtilis* b213 and A1/3. Chem. Biol. *6*, 31–41.
23. Toyota, K., and Kimura, M. (1993). Colonization of chlamydospores of *Fusarium oxysporum f. sp. raphani* by soil bacteria and their effects on germination. Soil Biol. Biochem. *25*, 193–197.
24. Lin, X., and Heitman, J. (2005). Chlamydospore formation during hyphal growth in *Cryptococcus neoformans*. Eukaryot. Cell *4*, 1746–1754.
25. Álvarez, B., Biosca, E.G., and López, M.M. (2010). On the life of *Ralstonia solanacearum*, a destructive bacterial plant pathogen. In Current Research, Technology and Education Topics in Applied Microbiology and Microbial Biotechnology, Second Edition, A. Méndez-Vilas, ed. (Formatex Research Center)), pp. 267–279.
26. van Elsas, J.D., Kastelein, P., van Bekkum, P., van der Wolf, J.M., de Vries, P.M., and van Overbeek, L.S. (2000). Survival of *Ralstonia solanacearum* biovar 2, the causative agent of potato brown rot, in field and microcosm soils in temperate climates. Phytopathology *90*, 1358–1366.
27. Kong, H.G., Bae, J.Y., Lee, H.J., Joo, H.J., Jung, E.J., Chung, E., and Lee, S.-W. (2014). Induction of the viable but nonculturable state of *Ralstonia solanacearum* by low temperature in the soil microcosm and its resuscitation by catalase. PLoS One *9*, e109792.
28. Nemergut, D.R., Schmidt, S.K., Fukami, T., O'Neill, S.P., Bilinski, T.M., Stanish, L.F., Knelman, J.E., Darcy, J.L., Lynch, R.C., Wickey, P., and Ferrenberg, S. (2013). Patterns and processes of microbial community assembly. Microbiol. Mol. Biol. Rev. *77*, 342–356.
29. Biniarz, P., Łukaszewicz, M., and Janek, T. (2017). Screening concepts, characterization and structural analysis of microbial-derived bioactive lipopeptides: a review. Crit. Rev. Biotechnol. *37*, 393–410.
30. Mondol, M.A.M., Shin, H.J., and Islam, M.T. (2013). Diversity of secondary metabolites from marine *Bacillus* species: chemistry and biological activity. Mar. Drugs *11*, 2846–2872.

31. Li, L., Ma, M., Huang, R., Qu, Q., Li, G., Zhou, J., Zhang, K., Lu, K., Niu, X., and Luo, J. (2012). Induction of chlamydospore formation in Fusarium by cyclic lipopeptide antibiotics from *Bacillus subtilis* C2. J. Chem. Ecol. *38*, 966–974.

32. Sur, S., Romo, T.D., and Grossfield, A. (2018). Selectivity and mechanism of fengycin, an antimicrobial lipopeptide, from molecular dynamics. J. Phys. Chem. B *122*, 2219–2226.

33. Liang, X., Nong, X.-H., Huang, Z.-H., and Qi, S.-H. (2017). Antifungal and antiviral cyclic peptides from the deep-sea-derived fungus *Simplicillium obclavatum* EIODSF 020. J. Agric. Food Chem. *65*, 5114–5121.

34. Nielsen, T.H., Christophersen, C., Anthoni, U., and Sørensen, J. (1999). Viscosinamide, a new cyclic depsipeptide with surfactant and antifungal properties produced by *Pseudomonas fluorescens* DR54. J. Appl. Microbiol. *87*, 80–90.

35. Nielsen, T.H., Thrane, C., Christophersen, C., Anthoni, U., and Sørensen, J. (2000). Structure, production characteristics and fungal antagonism of tensin - a new antifungal cyclic lipopeptide from *Pseudomonas fluorescens* strain 96.578. J. Appl. Microbiol. *89*, 992–1001.

36. Denning, D.W. (1997). Echinocandins and pneumocandins–a new antifungal class with a novel mode of action. J. Antimicrob. Chemother. *40*, 611–614.

37. Estes, K.E., Penzak, S.R., Calis, K.A., and Walsh, T.J. (2009). Pharmacology and antifungal properties of anidulafungin, a new echinocandin. Pharmacotherapy *29*, 17–30.

38. NCI Thesaurus Natl. Cent. Biotechnol. Information. PubChem Database Micafungin, CID=477468.

39. Petraitis, V., Petraitiene, R., Groll, A.H., Roussillon, K., Hemmings, M., Lyman, C.A., Sein, T., Bacher, J., Bekersky, I., and Walsh, T.J. (2002). Comparative antifungal activities and plasma pharmacokinetics of Micafungin (FK463) against disseminated candidiasis and invasive pulmonary aspergillosis in persistently neutropenic rabbits. Antimicrob. Agents Chemother. *46*, 1857–1869.

40. Smith, P., and Schuster, M. (2019). Public goods and cheating in microbes. Curr. Biol. *29*, R442–R447.

41. Champomier-Vergès, M.-C., Stintzi, A., and Meyer, J.-M. (1996). Acquisition of iron by the non-siderophore-producing Pseudomonas fragi. Microbiology (Reading) *142*, 1191–1199.

42. Sexton, D.J., and Schuster, M. (2017). Nutrient limitation determines the fitness of cheaters in bacterial siderophore cooperation. Nat. Commun. *8*, 230.

43. Cochrane, S.A., and Vederas, J.C. (2016). Lipopeptides from *Bacillus* and *Paenibacillus* spp.: A gold mine of antibiotic candidates. Med. Res. Rev. *36*, 4–31.

44. Reynolds, K.A., Luhavaya, H., Li, J., Dahesh, S., Nizet, V., Yamanaka, K., and Moore, B.S. (2018). Isolation and structure elucidation of lipopeptide antibiotic taromycin B from the activated taromycin biosynthetic gene cluster. J. Antibiot. (Tokyo) *71*, 333–338.

45. Kubicki, S., Bollinger, A., Katzke, N., Jaeger, K.E., Loeschcke, A., and Thies, S. (2019). Marine biosurfactants: biosynthesis, structural diversity and biotechnological applications. Mar. Drugs *17*, 408.

46. Götze, S., and Stallforth, P. (2020). Structure, properties, and biological functions of nonribosomal lipopeptides from pseudomonads. Nat. Prod. Rep. *37*, 29–54.

47. Zhao, P., Xue, Y., Li, X., Li, J., Zhao, Z., Quan, C., Gao, W., Zu, X., Bai, X., and Feng, S. (2019). Fungi-derived lipopeptide antibiotics developed since 2000. Peptides *113*, 52–65.

48. Aleti, G., Sessitsch, A., and Brader, G. (2015). Genome mining: prediction of lipopeptides and polyketides from *Bacillus* and related Firmicutes. Comput. Struct. Biotechnol. J. *13*, 192–203.

49. Xu, B.-H., Lu, Y.-Q., Ye, Z.-W., Zheng, Q.-W., Wei, T., Lin, J.-F., and Guo, L.-Q. (2018). Genomics-guided discovery and structure identification of cyclic lipopeptides from the *Bacillus siamensis* JFL15. PLoS One *13*, e0202893.

50. Esmaeel, Q., Pupin, M., Kieu, N.P., Chataigné, G., Béchet, M., Deravel, J., Krier, F., Höfte, M., Jacques, P., and Leclère, V. (2016). *Burkholderia* genome mining for nonribosomal peptide synthetases reveals a great potential for novel siderophores and lipopeptides synthesis. Microbiologyopen *5*, 512–526.

51. Stincone, P., Veras, F.F., Pereira, J.Q., Mayer, F.Q., Varela, A.P.M., and Brandelli, A. (2020). Diversity of cyclic antimicrobial lipopeptides from *Bacillus* P34 revealed by functional annotation and comparative genome analysis. Microbiol. Res. *238*, 126515.

52. Zhao, H., Liu, Y.-P., and Zhang, L.-Q. (2019). *In silico* and genetic analyses of cyclic lipopeptide synthetic gene clusters in *Pseudomonas* sp. 11K1. Front. Microbiol. *10*, 544.

53. Cole, G.T., Seshan, K.R., Phaneuf, M., and Lynn, K.T. (1991). Chlamydospore-like cells of *Candida albicans* in the gastrointestinal tract of infected, immunocompromised mice. Can. J. Microbiol. *37*, 637–646.

54. Schäfer, K., Di Pietro, A., Gow, N.A.R., and MacCallum, D. (2014). Murine model for *Fusarium oxysporum* invasive fusariosis reveals organ-specific structures for dissemination and long-term persistence. PLoS One *9*, e89920.

55. Chabasse, D., Bouchara, J.P., de Gentile, L., and Chennebault, J.M. (1988). Chlamydospores de *Candida albicans* observées *in vivo* chez un patient atteint de Sida [*Candida albicans* chlamydospores observed *in vivo* in a patient with AIDS]. Ann. Biol. Clin. (Paris) *46*, 817–818.

56. Baum, G.L. (1960). The significance of *Candida albicans* in human sputum. N. Engl. J. Med. *263*, 70–73.

57. Kimura, M., Nishimura, K., Enoki, E., Chikugo, T., and Maenishi, O. (2012). Chlamydospores of *Rhizopus microsporus* var. rhizopodiformis in tissue of pulmonary mucormycosis. Mycopathologia *174*, 441–450.

58. Nazir, R., Warmink, J.A., Boersma, H., and Van Elsas, J.D. (2010). Mechanisms that promote bacterial fitness in fungal-affected soil microhabitats. FEMS Microbiol. Ecol. *71*, 169–185.

59. Desirò, A., Salvioli, A., Ngonkeu, E.L., Mondo, S.J., Epis, S., Faccio, A., Kaech, A., Pawlowska, T.E., and Bonfante, P. (2014). Detection of a novel intracellular microbiome hosted in arbuscular mycorrhizal fungi. ISME J *8*, 257–270.

60. Boucher, C.A., Van Gijsegem, F., Barberis, P.A., Arlat, M., and Zischek, C. (1987). *Pseudomonas solanacearum* genes controlling both pathogenicity on tomato and hypersensitivity on tobacco are clustered. J. Bacteriol. *169*, 5626–5632.

61. Tran, T.M., MacIntyre, A., Hawes, M., and Allen, C. (2016). Escaping underground nets: extracellular DNases degrade plant extracellular traps and contribute to virulence of the plant pathogenic bacterium *Ralstonia solanacearum*. PLoS Pathog *12*, e1005686.

62. Kroken, A.R., Chen, C.K., Evans, D.J., Yahr, T.L., and Fleiszig, S.M.J. (2018). The impact of ExoS on *Pseudomonas aeruginosa* internalization by epithelial cells is independent of fleQ and correlates with bistability of type three secretion system gene expression. mBio *9*, 668–686.

63. Wiles, T.J., Bower, J.M., Redd, M.J., and Mulvey, M.A. (2009). Use of zebrafish to probe the divergent virulence potentials and toxin requirements of extraintestinal pathogenic *Escherichia coli*. PLoS Pathog *5*, e1000697.

64. Tancos, M.A., Lowe-Power, T.M., Peritore-Galve, F.C., Tran, T.M., Allen, C., and Smart, C.D. (2018). Plant-like bacterial expansins play contrasting roles in two tomato vascular pathogens. Mol. Plant Pathol. *19*, 1210–1221.

65. Vincent, W.J.B., Freisinger, C.M., Lam, P.-Y., Huttenlocher, A., and Sauer, J.-D. (2016). Macrophages mediate flagellin induced inflammasome activation and host defense in zebrafish. Cell. Microbiol. *18*, 591–604.

66. Riddell, R.W. (1950). Permanent stained mycological preparations obtained by slide culture. Mycologia *42*, 265–270.

67. Dereeper, A., Guignon, V., Blanc, G., Audic, S., Buffet, S., Chevenet, F., Dufayard, J.-F., Guindon, S., Lefort, V., Lescot, M., et al. (2008). Phylogeny.fr: robust phylogenetic analysis for the non-specialist. Nucleic Acids Res *36*, W465–W469.

STAR★METHODS

KEY RESOURCES TABLE

REAGENT or RESOURCE	SOURCE	IDENTIFIER
Bacterial and virus strains		
Ralstonia solanacearum GMI1000	Boucher et al.[60]	N/A
Ralstonia solanacearum GMI1000 Δ*rmyA*	Spraker et al.[13]	N/A
Ralstonia solanacearum GMI1000 GFP	Tran et al.[61]	N/A
Ralstonia solanacearum GMI1000 dsRed	Dr. Caitilyn Allen, UW-Madison	N/A
Ralstonia solanacearum GMI1000 Δ*rmyA* GFP	Spraker et al.[13]	N/A
Pseudomonas aeruginosa PaO1 GFP	Kroken et al.[62]	N/A
Escherichia coli UTI89 GFP	Wiles et al.[63]	N/A
Herbaspirillum seropedicae B3 GFP	Dr. Jean Michel Ané, UW-Madison	N/A
Clavibacter michiganensis 0317 GFP	Tancos et al.[64]	N/A
Listeria monocytogenes 10403S mCherry	Vincent et al.[65]	N/A
Methicillin resistant *Staphylococcus aureus* strain FPR3757LAC dsRed	John Demian Sauer, UW-Madison	N/A
Bacillus velezensis Y6	Cao et al.[20]	N/A
Bacillus velezensis Y6 Δ*fenC*	Cao et al.[20]	N/A
Biological samples		
Aspergillus flavus NRRL 3357	American Type Culture Collection	ATCC 200026
Fusarium oxysporum f. sp. *lycopersici* 4287	Dr. Antonio Di Pietro, Universidad de Cordoba	N/A
Chemicals, peptides, and recombinant proteins		
Bacto™ Yeast Extract	BD	Cat. # 212750
Bacto™ Peptone	BD	Cat. # 211677
Casein, Acid Hydrolysate	Sigma-Aldrich	Cat # 65072-00-6
Dextrose	Fisher	Cat. # D16-500
Agar	Fisher	Cat. # AAJ10654Q1
Sodium Chloride	Fisher	Cat. # 7647-14-5
Bacto™ Tryptic Soy Broth	BD	Cat. # 211825
Brain Heart Infusion Broth	Sigma-Aldrich	Cat. # 53286-100G
Dehydrated Culture Media: Potato Dextrose Broth	BD Difco	Cat. # 213300
Calcofluor White Stain	Sigma-Aldrich	Cat. # 18909-100ML-F
Cycloheximide	Fisher	Cat. # AC35742-0050
Ampicillin	Goldbio	Cat. # A-301-5
Deposited data		
Raw data deposited on Mendeley.	This paper	https://doi.org/10.17632/hv528mtmm5.1
Staphylococcus aureus strain ATCC 12600 16S ribosomal RNA, complete sequence	NCBI	Accession number NR_118997.2
Pseudomonas aeruginosa strain PAO1 16S ribosomal RNA gene, partial sequence	NCBI	Accession number DQ777865.1
Herbaspirillum sp. B501 gene for 16S rRNA, partial sequence	NCBI	Accession number AB049133.1
L. monocytogenes DNA for 16S ribosomal RNA	NCBI	Accession number X98530.1

(*Continued on next page*)

Continued

REAGENT or RESOURCE	SOURCE	IDENTIFIER
Clavibacter michiganensis subsp. *michiganensis* strain Cmm VT3 16S ribosomal RNA gene, partial sequence	NCBI	Accession number HQ144242.1
Ralstonia solanacearum GMI1000 strain GMI1000 16S ribosomal RNA, complete sequence	NCBI	Accession number NR_074551.1
rrsB (*Escherichia coli str. K-12 substr. MG1655*)	NCBI	Accession number NC_000913.3 positions (4166659-4168200)
(Mycetohabitans rhizoxinica) Burkholderia rhizxinica 16S rRNA gene, type strain HKI 454T	NCBI	Accession number AJ938142.1
Candidatus Glomeribacter gigasporarum 16S rRNA gene (from G. margarita strain WV205A-5)	NCBI	Accession number AJ251633.1
(*Mycetohabitans endofungorum*) Burkholderia endofungorum 16S rRNA gene, type strain HKI 456T	NCBI	Accession number AM420302.1
Klebsiella pneumoniae strain DSM 30104 16S ribosomal RNA, partial sequence	NCBI	Accession number NR_036794.1
Acinetobacter baumannii strain DSM 30007 16S ribosomal RNA, partial sequence	NCBI	Accession number NR_026206.1
Salmonella enterica subsp. *arizonae* strain ATCC 13314 16S ribosomal RNA, partial sequence	NCBI	Accession number NR_041696.1
Bacillus subtilis strain IAM 12118 16S ribosomal RNA, complete sequence	NCBI	Accession number NR_112116.2
Agrobacterium tumefaciens strain IAM 12048 16S ribosomal RNA, partial sequence	NCBI	Accession number NR_041396.1
Uncultured *Bradyrhizobium* sp. gene for 16S ribosomal RNA, partial sequence, clone: THIF01sym.	DDBJ	Accession number AB474797
Uncultured bacterium isolate EH-9054 16S ribosomal RNA gene, partial sequence	NCBI	Accession number HM117724.1
Serratia marcescens strain D1 16S ribosomal RNA gene, partial sequence	NCBI	Accession number MF893336.1
Neisseria meningitidis strain M1027 16S ribosomal RNA, partial sequence	NCBI	Accession number NR_104946.1
(*Candidatus* Mycoavidus necroximicus) Bacterium endosymbiont of *Podila verticillata* CBS 315.52 clone BRE315.52 16S ribosomal RNA gene, partial sequence	NCBI	Accession number MZ330687.1
(*Chitinophaga* sp.) Uncultured bacterium clone EHB-PS0362 16S ribosomal RNA gene, partial sequence	NCBI	Accession number KU978322.1
Software and algorithms		
Nikon NIS Elements AR software package (Version 4.13)	Nikon	N/A
Nikon NIS Elements AR Analysis package (Version 4.13)	Nikon	N/A
Fiji (Version 2.0.0-rc-69)	ImageJ	N/A
GraphPad Prism (Version 8.3.0)	GraphPad	N/A
TRILUTION LC (Version 3.0)	Gilson	N/A
Phylogeny.fr	www.phylogeny.fr	N/A
Other		
Nikon Eclipse Ti inverted microscope	Nikon	N/A
Nikon Plan Fluor lens system	Nikon	N/A

(*Continued on next page*)

Continued

REAGENT or RESOURCE	SOURCE	IDENTIFIER
Heated microscope enclosure	OKO Labs	N/A
Nalgene™ Rapid-Flow™ Filter Units	Thermo Scientific	Cat. # 155-0020
Sorvall RC 6 Plus centrifuge	Thermo Scientific	Cat. # 12121680
171 Gilson Diode Array Detector	Gilson	N/A
Gilson GX-271 Liquid Handler	Gilson	N/A
Zorbax Eclipse XDB-C18 column	Zorbax	N/A
Thermo Scientific-Vanquish UHPLC	Thermo Scientific	N/A
Thermo Scientific Q Exactive Orbitrap mass spectrometer	Thermo Scientific	N/A

RESOURCE AVAILABILITY

Lead contact

Further information and requests for resources and reagents should be directed to and will be fulfilled by the lead contact, Dr. Nancy Keller (npkeller@wisc.edu).

Materials availability

This study did not generate any new unique reagents. All strains will be provided from the Keller Lab upon request.

Data and code availability

- All data is available in the main text or the supplementary materials. Videos are provided as.mov files. All raw data were deposited on Mendeley at https://doi.org/10.17632/hv528mtmm5.1 repository and is publicly available as of the date of publication.
- This paper does not report original code.
- Any additional information required to reanalyze the data reported in this paper is available from the lead contact upon request.

EXPERIMENTAL MODEL AND SUBJECT DETAILS

Strains and culture conditions

All fungal and bacterial strains used in the study and their sources are listed in the key resources table. All strains were stored at -80° C in 33% glycerol. When needed, bacterial strains were streaked out in media optimal to each bacterium and incubated at 30 °C for 1-2 days. *R. solanacearum* was routinely grown in CPG medium, amended with 0.005% Tetrazolium chloride. *P. aeruginosa*, *E. coli*, and *S. aureus* were grown in Lysogeny Broth (LB) medium. *H.* seropedicae was grown in Tryptic Soy Agar (TSA). *L. monocytogenes* was grown in Brain Heart Infusion (BHI) medium. *A. flavus* was grown on GMM at 30 °C for 5 days. F. oxysporum was grown on Potato Dextrose Agar (PDA) at 30 °C for 5 days. All bacterial strains were freshly grown from glycerol stocks for every experiment.

Media recipes

CPG (1L): 1 g Casamino acids, 1 g Bacto™ Yeast Extract, 10 g Dextrose, 10 g Bacto™ Peptone, 16g agar

LB (1L): 5 g Bacto™ Yeast Extract, 10 g Bacto™ Peptone, 10 g Sodium Chloride, pH 7.0

TSA: Bacto™ Tryptic Soy Broth, 16 g/L Agar

BHI: Sigma Aldrich Brain Heart Infusion Broth, 16 g/L Agar

GMM (1 L): 50ml 20X Nitrate salts, 1 mL Trace elements, 10 g Dextrose, 16 g Agar, pH 6.5.

20X Nitrate Salts (1L): 120 g $NaNO_3$, 10.4 g KCl, 10.4 g $MgSO_4.7H_2O$, 30.4 g KH_2PO_4

Trace Elements (100 mL): 2.2 g $ZnSO_4.7H_2O$, 1.1 g H_3BO_3, 0.5 g $MnCl_2.4H_2O$, 0.5 g $FeSO_4.7H_2O$, 0.16 g $CoCl_2.5H_2O$, 0.16 g $CuSO_4.5H_2O$, 0.11 g $(NH_4)_6Mo_7O_{24}.4H_2O$, 5 g Na_4EDTA

BMM (1L): 3.4 g KH2PO4, 0.5 g $(NH_4)_2SO_4$,100 microliters of 1.25 mg/mL stock solution $FeSO_4$ $7H_2O$, 517 microliters of 1 M stock solution $MgSO_4$, 2 g Dextrose, pH 6.5.

PDA (1 L): BD Difco™ Dehydrated Culture Media: Potato Dextrose Broth, 16 g/L Agar

PDB (1 L): BD Difco™ Dehydrated Culture Media: Potato Dextrose Broth

Inoculum preparation

Single bacterial colonies were raised in 4 mL liquid CPG overnight at 30 °C with constant shaking at 250 rpm, washed 3 times with sterile double distilled water and diluted as needed. *A. flavus* spores were harvested from GMM plates incubated for 5 days at 30 °C

with 0.001% Tween and diluted as required. To raise microconidia from *F. oxysporum*, a fungal plug was inoculated into 50 mL Potato Dextrose Broth (PDB) and incubated at 30 °C with continuous shaking at 250 rpm for 5 days. The culture was then filtered with a double-layered Miracloth™ to obtain spores as the filtrate, washed 2X with sterile double distilled water and resuspended in 1/10th volume. Conidia were counted on a hemocytometer, stored at 4 °C, and used up to two weeks.

METHOD DETAILS

Supernatant collection

Supernatant from *R. solanacearum* was collected as follows. A single mucoid bacterial colony freshly grown from glycerol stock was inoculated into liquid CPG and incubated at 28 °C, overnight with constant shaking at 250 rpm. 1 mL of overnight culture was inoculated into 250 mL of CPG in a 500 mL conical flask and grown for 24 hours. The culture was centrifuged at 10000 rpm in the Sorvall RC 6 Plus centrifuge for 10 minutes to pellet the cells and the supernatant was filtered with a 0.2 μm Nalgene™ Rapid-Flow™ vacuum filtration setup. The supernatant was stored at -80 °C in aliquots until use. Supernatant from *B. velezensis* cultures were collected as described elsewhere.[20]

Co-culture setup for colonization assessment

For live imaging of *A. flavus* chlamydospore formation in response to *R. solanacearum* supernatant, *A. flavus* spores (1000 spores/well in a 96-well plate) were incubated in 100 μL GMM for 8 hours at 30 °C. 100 μL of supernatant was then added to each well and images were taken every 2 hours for 24 hours. The samples were incubated at 30 °C for 24 h in a heated microscope enclosure (OKO Labs, Burlingame, CA) developed for a Nikon Eclipse Ti inverted microscope. To characterize concentration dependence of chlamydospore formation to purified RM, the same setup described above was used with the following variations: 100 μL of supernatant was replaced with 90 μl of GMM and 10 μl of RM of varying concentrations as shown in Figure 1B. The setup was incubated for 48 hours at 30 °C, washed 2X with GMM, stained for 5 minutes with 0.1 mg/mL calcofluor white, washed 2X with GMM and imaged. 2 replicates were assessed for each concentration with 6 frames per replicate (set in a 10 μm x 5 μm rectangle). Propidium iodide staining was done at 25 μg/mL for 5 minutes and washed 2 times with equal volume of sterile double distilled water before being mounted on slides for imaging in the RFP channel. For analysis of RM induced macroscopic changes on A. flavus, 10 μL of 10^5 spores/mL *A. flavus* spores was spotted on CPG 1.5 cm away from 10 μL of RM spots at the concentrations shown in Figure 1C. The plates were incubated for 4 days at 30 °C and the interaction zones (5 mm x 2 mm) were excised, stained with 0.1 mg/mL calcofluor white and imaged. 4 replicates were imaged per concentration and 6 frames were imaged per replicate.

For co-cultures of bacteria with *A. flavus* for imaging purposes, *A. flavus* spores were overlaid in CPG at a concentration of 10^7 spores in 30 mL and incubated at 30 °C for ~14 hours. The experimental setup is adapted from Riddell mounts,[66] illustrated with schematics in Figure S1C. Each fungal plug was topped with 100 μL of bacteria (final OD=0.025) mixed with *R. solanacearum* supernatant, ralsolamycin and/or methanol, before placing a sterile cover slip on top. All imaging analyses were independently repeated at least two times. For three-way co-cultures, *R. solanacearum* and *P. aeruginosa* were mixed in equal proportions, each to a final OD=0.0125 before addition to the fungal plug. Invasion was assessed for at least 4 replicates in each independent experiment, where at least 25 colonized chlamydospores were observed. Data from the 4 technical replicates were pooled to calculate % chlamydospores colonized. Experiments were repeated independently 2-4 times. The setup was incubated at 30 °C for 48 hours and then imaged as detailed in the section below. ODs for all bacterial cultures were monitored at 600 nm.

Imaging and image processing

All imaging analyses were performed on Nikon Eclipse Ti inverted microscope. Chlamydospore colonization by bacteria was assessed with z-stack imaging (automated and manual), performed at 20 X and 60 X with the Nikon Plan Fluor lens system controlled by the Nikon NIS Elements AR software package (Version 4.13) in Phase Contrast or Differential Interference Contrast mode in the GFP, RFP or DAPI (for calcofluor white stained samples) channels as appropriate. The top and the bottom of each chlamydospore was manually set and image of slices 3 μm apart were obtained. The fluorescence of every point along a given path (Figure S3C) was assessed with the Nikon NIS Elements AR Analysis package v4.13. The z-stack image files were loaded on to Fiji version 2.0.0-rc-69. Chlamydospores with bacteria in more than 3 slices were categorized as being colonized and at least four individuals assessed colonization for all experiments in a blind test For depth color code, the fluorescent images were loaded and 8-12 frames in focus were color coded with the 'Temporal Color Code' option in 'Hyperstacks' with the 'Royal' color scale available on Fiji.

Bacterial recovery from fungal mycelia

Co-cultures were washed with sterile double distilled water 5 times and homogenized with a bead beater with 0.5 mm silica beads. The homogenate was then serially diluted and plated on CPG+130 μg/mL cycloheximide to select for and quantify viable bacterial colony forming units. Homogenate from cold stressed *R. solanacearum* cells and pure cultures were treated with 1000 U/mL catalase in the dark for 3 days at 30 °C, before serially diluted and plated on bacterial selective media. The plates were incubated at 30 °C for 1-2 days and Colony Forming Units (CFUs) were counted. For all bacterial recovery analyses, 3-4 independent experiments were performed. 4-6 replicates were set up for each independent experiment and three co-culture mycelial mats were pooled for each replicate.

Stress tests

For all abiotic stress tests, the co-cultures were set up in 96-well plates, with directions for each well as follows. For *R. solanacearum-A. flavus* co-cultures, 1 million spores were incubated in 190 μL of CPG overnight at 30 °C, and 10 μL of bacteria grown overnight was added the next morning to a final OD=0.001. The setup was incubated at 30C for 48 hours. For *P. aeruginosa-A. flavus* and *L.monocytogenes-A.flavus* co-cultures with *R. solanacearum* supernatants, 1 million spores were incubated in 150 μL of CPG overnight at 30 °C. Post incubation, 10 μL of bacteria grown overnight in CPG and 40 μL of supernatant was added. The bacteria were added to result in a final OD=0.0001 for *P. aeruginosa* and OD=0.005 for *L. monocytogenes* in 200 μL. The setup was incubated at 30 °C for 48 hours. The mycelial mats were washed with sterile double distilled water 5 times, dried with filter paper and transferred into the required conditions, as described below. For *R. solanacearum* pure culture controls, cells grown overnight were inoculated into appropriate conditions (described below) to a final OD=0.025 and incubated at 30 °C for 48 hours. *P. aeruginosa* and *L. monocytogenes* were inoculated at a final OD of 0.005 in 0.25X *R.solanacearum* supernatant for 48 hours, collected, washed, and then placed under appropriate medium at a final OD of 0.01. For all stress tests, at least two independent experiments were performed for all co-cultures.

To induce nutrient stress, *R. solanacearum* co-cultures and pure cultures were placed in sterile double distilled water and *P. aeruginosa* co-cultures and pure cultures were incubated in Corning® Phosphate Buffered Saline pH 7.0. Boucher's minimal medium (BMM) was used as the control. Cultures were incubated for 48 hours at 30 °C. For cold stress, cultures were incubated in BMM at 4 °C for 28 days with 30 °C cultures as the control. Post stress, bacteria were recovered from the fungal mycelia as described in the "bacterial recovery from fungal mycelia" section. Pure cultures were serially diluted and plated on bacterial selective media.

For analysis of chlamydospore formation and invasion by starved *R. solanacearum* cells, overnight cultures were inoculated at a final OD=0.025 and incubated for 48 hours in sterile double distilled water. The cells were then centrifuged, pelleted, and concentrated and then added to co-cultures as described in the "co-culture setup for colonization assessment" section. Chlamydospores were counted as described in the "co-culture setup for colonization assessment" section. Starved cells were washed and resuspended in WT *R. solanacearum* supernatant to assess invasion in the presence of exogenous RM.

R. solancearum overwintering in soil microcosms

Soil microcosm was set up as shown in Figure S1B with autoclaved potting soil. Post cold stress, the soil in each Petri dish was thoroughly mixed and ~0.1 g of soil was transferred to 10 mL of 0.01% agar. The mixture was vortexed, serially diluted and plated on CPG+130 μg/mL cycloheximide (bacterial-selective) and PDA+100 μg/mL Ampicillin (fungal selective). The plates were incubated at 30 °C for 1-2 days and CFUs were counted.

Chromatographic techniques

Purified RM was resuspended in LCMS-grade methanol to a final concentration of 1.25 M and then diluted to 1 mg/mL in a mixture of LCMS-grade 80% Acetonitrile and 20% water. The compound was analyzed with HPLC-DAD and UPLC-HRMS.

HPLC-DAD was performed on Gilson GX-271 Liquid Handler with system 322 H2 Pump connected to a 171 Gilson Diode Array Detector. The XBridge C18 3.5 μm, 4.6x150 mm column was used for the analytical run with a flow rate of 0.8 mL/min. HPLC grade water with 0.5% formic acid (solvent A) and HPLC grade acetonitrile with 0.5% formic acid (solvent B) were used with the gradient: 0 min, 20% Solvent B; 2 min, 20% Solvent B; 15 min, 95% Solvent B; 20 min, 95% Solvent B; 20 min, 20% Solvent B; 25 min, Solvent B. Data acquisition and analysis for the HPLC-DAD were performed with TRILUTION LC V3.0.

UHPLC-HRMS was performed on a Thermo Scientific-Vanquish UHPLC system connected to a Thermo Scientific Q Exactive Orbitrap mass spectrometer in ES^+ and ES^- mode between 200 m/z and 1400 m/z to identify metabolites. A Zorbax Eclipse XDB-C18 column (2.1 × 150 mm, 1.8 μm 123 particle size) was used with a flow rate of 0.2 mL/min. LCMS grade water with 0.5% formic acid (solvent A) and LCMS grade acetonitrile with 0.5% formic acid (solvent B) were used with the gradient: 0 min, 20% Solvent B; 2 min, 20% Solvent B; 15 min, 95% Solvent 126 B; 20 min, 95% Solvent B; 20 min, 20% Solvent B; 25 min, Solvent B. Data acquisition and analysis for the UHPLC-MS were performed with Thermo Scientific Xcalibur software Version 3.1.66.10.

Phylogenetic analyses

The phylogenetic trees in Figures 2C and S3E were constructed with phylogeny.fr.[67] with default parameters in the 'One-click mode'. The analysis is performed with 16S rRNA sequences whose NCBI Accession details are presented in the key resources table.

QUANTIFICATION AND STATISTICAL ANALYSIS

All statistical analyses were performed with GraphPad Prism version 8.3.0. Outliers were identified with ROUT=0.5%. Model fit was assessed with QQ plots, residual plots and by testing normality of residuals with Anderson-Darling (A2*), D'Agostino-Pearson omnibus (K2), Shapiro-Wilk (W), or Kolmogorov-Smirnov (distance) tests. One representative dataset for each type of experiment conducted in this study is chosen, and the set of tests performed to identify the appropriate statistical model is detailed in Data S1. In cases where distribution was normal and model fit was validated, unpaired t-tests with Welch's correction, one-way ANOVA, or two-way ANOVA were performed as appropriate with relevant post hoc analyses (as indicated in figure legends). For assessment of endofungal bacterial fitness, two-way ANOVA was performed to identify interaction of supernatant treatment x

nutrient condition. In cases, where the distribution was non-normal, non-parametric tests were performed. The tests performed for each dataset is detailed in corresponding figure legends. For soil microcosm experiments, N=3 and normality tests could not be performed as N was too small. Therefore, a normal distribution of the data was assumed and an unpaired t-test with Welch's correction was performed. Two data points in 'Rs' treatment were below detection limit (noted in the figure) and these values were substituted with ½ value of limit of detection for statistical analysis.